Segmented design and control in contra-directional coupler for large bandwidth tunability

Segmented Design and Control in Contra-Directional Couplers for Large Bandwidth Tunability

Lorenzo Tunesi[a], Mohammad Amin Mahdian[b], Andrea Carena[a], Vittorio Curri[a], Mahdi Nikdast[b], and Paolo Bardella[a]

[a]Department of Electronic and Telecommunications, Politecnico di Torino, Torino, Italy
[b]Department of Electrical and Computer Engineering, Colorado State University, Fort Collins, CO, USA

ABSTRACT

We propose a novel design and control mechanism to achieve a widely tunable add-drop filtering element based on silicon photonic Grating-Assisted Contra-Directional Couplers. The proposed device has been simulated considering integration on the silicon photonics platform, allowing for wide deployment and cost-effective implementation as an integrated building block for different filtering/switching applications (e.g., multiplexers and demultiplexers). The segmented design and optimization of the coupler have been shown to enable a large drop bandwidth tunability while keeping a constant central wavelength, avoiding channel drifts. This add-drop element can be envisioned for flex-band wavelength-division multiplexing (WDM) applications as a component of wavelength-selective switches (WSS) or other switching devices.

Keywords: Tunable bandwidth, grating-assisted contra-directional couplers, chirped gratings, silicon photonics

1. INTRODUCTION

Grating-Assisted Contra-Directional Couplers (CDCs) are extremely versatile integrated photonic devices that can benefit a wide range of applications, from tunable reflectors and add-drop filters to mode multiplexers and converters. This is possible due to their flexible design space and large degree of freedom, allowing customization to satisfy specific application requirements. At their core operation, they are four-port devices enabling frequency-selective add-drop filtering by means of Bragg's grating structures, which allow for the coupling of forward and backward propagating modes of the two waveguides (Fig. 1a). Starting from an uncoupled asymmetric two waveguide system, by adding a periodic perturbation of the waveguides widths we can introduce wavelength-selective coupling, leveraging the asymmetry between the unperturbed waveguide size and the grating period and geometry.[1]

In the traditional two-waveguide configuration, part of the spectrum of the input field is coupled to the backward port of the second waveguide, another spectral slice is instead reflected backward to the same input port while the rest of the signal travels to the output port of the input waveguide. The transfer function is defined by the geometric properties of the waveguides, while the add-drop channel frequency is determined by the periodic perturbation of the waveguides, and in particular by the phase-match intersection between the average waveguide index and the Bragg's pitch (Λ). More complex coupling effects can be introduced by properly matching the geometries of the waveguide resulting in a versatile design space.[2] Moreover, CDCs have also been implemented in the silicon photonics platform with great success.[3,4] Their technological maturity together with their flat-top wideband filtering response make them competitive devices for signal processing and optical telecommunication switching and filtering applications[5–7] .

In this paper, we present a thermal-based control technique to increase bandwidth tunability in CDC filters while analyzing the maximum bandwidth tunability ranges and limiting factors. The simulation and design of CDCs have been carried out through well-established analytical models in the literature , with the material parameters and waveguide properties extracted from data obtained through the RSoft Photonic Simulation Suite.

Further author information: Lorenzo Tunesi.: E-mail: lorenzo.tunesi@polito.it

Optical Components and Materials XXI, edited by Shibin Jiang, Michel J. F. Digonnet, Proc. of SPIE Vol. 12882, 128820B
 · 0277-786X · doi: 10.1117/12.3002611

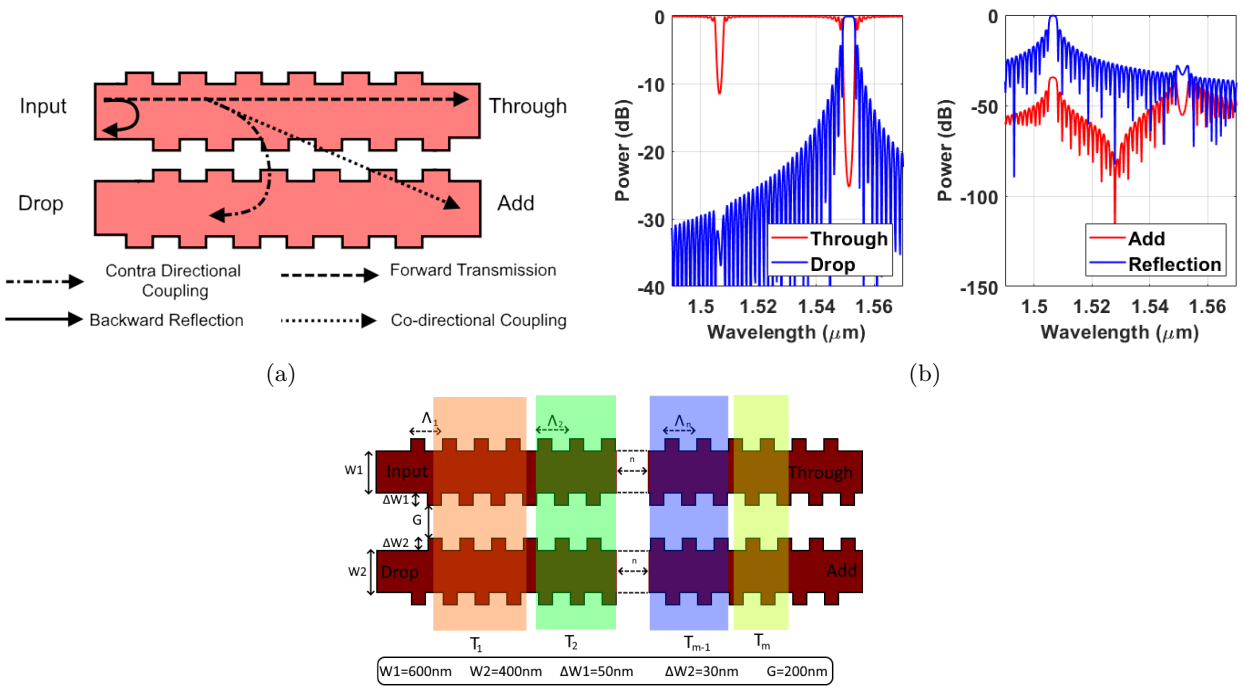

Figure 1: (a) Generic CDC device highlighting the four couplings experienced by the forward propagating input signal. (b) Frequency response at the four ports of a conventional CDC device, highlighting the desired response at the output ports (through and drop) as well as the parasitic unwanted effects (backward reflection to the input port and direct coupling at the add port). (c) Segmented CDC structure with reference waveguide geometry.

2. DESIGN OF GRATING-ASSISTED CONTRA-DIRECTIONAL COUPLERS

The device under analysis is a C-band CDC filter with central design frequency $\lambda = 1550\,\text{nm}$, demonstrating a bandwidth tunability range of $\Delta f_{3\text{dB}} \approx 610\,\text{GHz}$ from $f_{3\text{dB,min}} = 308\,\text{GHz}$ to $f_{3\text{dB,max}} = 924\,\text{GHz}$. Simulations have been carried out in MATLAB using the well established Coupled-Mode Theory (CMT),[1] which allows for simulations of arbitrary sized CDCs without requiring time consuming and computationally expensive methods, such as Finite-Difference Time-Domain (FDTD). The matrix-based approximation provided by the CMT model allows for a relatively accurate simulation of the device behavior, enabling the analysis of devices with longitudinal parameter variations, such as pitch, temperature, and coupling chirping.

The CMT model does not require any data on the waveguide geometry, as the simulation is carried out through parameters such as the effective index and coupling coefficients. Such waveguide simulations have been carried out in the RSoft Photonic Simulation Suite to extract reasonable values for both the effective index curves as well as the coupling coefficients of the device. Fig. 1c illustrates the general schematic of the structure, together with the geometric parameters considered for the two waveguides. The physical parameters have been selected to achieve the desired coupling coefficients and effective index curves, while maintaining a realistic geometry, validating the design through modal analysis and parameter extraction methods well established in the literature.[8]

The structure considered in our work is not a trivial CDC implementation, and it has been simulated considering a wide variety of optimization techniques to improve the performance and spectral response of the device. In addition, our device is controlled through a segmented micro-heater, allowing for thermal gradient configurations.[9] The typical response of a CDC device can be seen in Fig. 1b: the add-drop channel exhibits the correct flat-top behavior, although there are undesired side lobes as well as the intra-waveguide reflection peak. To improve the device performance, different design techniques can be deployed, starting from out-of-phase gratings that allow for minimization of the backward reflections, apodization of the grating profile to suppress the side

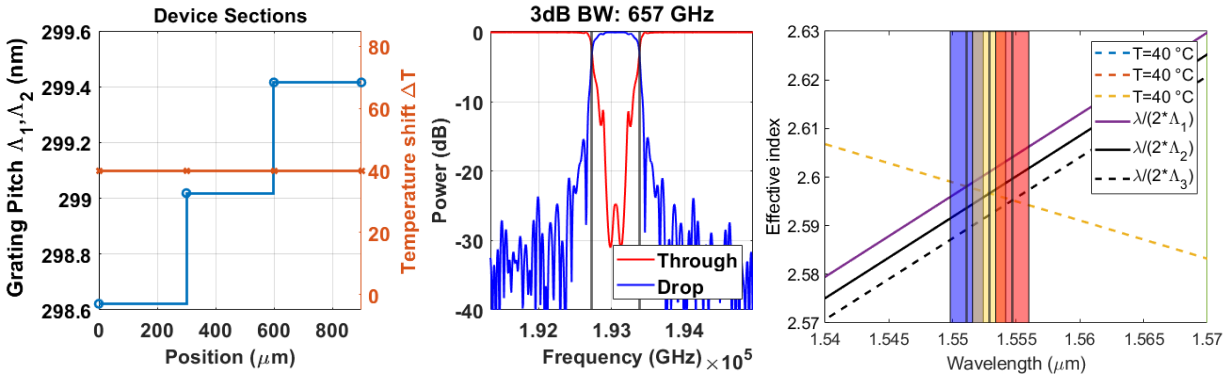

(a) Device regions and resulting response (b) Phase-match condition

Figure 2: Response of the three region segmented CDC under uniform thermal bias of T = 40 °C.

lobes, as well as pitch chirping[10] to increase the bandwidth. The CDC device under analysis has been designed considering all these techniques, and follows the same design principle described in our prior work in,[11] although targeting a slightly larger bandwidth: the device can be summarized as a pitch-chirped CDC with independent segmented thermal control, leveraging multiple regions with different grating period acting as a cascaded configuration to extend the static bandwidth and enhance the band thermal tunability, as will be discussed in the following section.

The parameters of the CMT model have been chosen to account for all these design choices and optimizations techniques, resulting in the coupling coefficients $\kappa_{11} = \kappa_{22} = 10\,\mathrm{cm}^{-1}$, $\kappa_{12} = 100\,\mathrm{cm}^{-1}$, three regions with pitches $\Lambda_{1-3} = [298.6, 299, 299.4]$nm over a total length of $L = 900\,\mu$m with a hyperbolic tangent apodization ($\alpha = 3,\ \beta = 3$). The number of regions has been reduced with respect to the previous work to offer a more reasonable tolerance margin with respect to manufacturing uncertainty, and to properly investigate the limits of the pitch-chirped enhanced bandwidth control: while in the previous work the device was comprised of more pitch regions, leading to a smoother transition, here we consider a larger step in the pitch variation, with a value between adjacent regions of $\Delta\Lambda = 0.4\,$nm. This allows a more accurate test of the proposed control scheme limits, as the larger step facilitates the formation of stop-bands or notches in the drop channel.
The response of the device is depicted in Fig. 2, with a uniform thermal shift applied to act as bias and allow a constant central wavelength in different control states. All temperatures depicted are considered as shifts from the ambient temperature. Fig. 2b depicts the phase-match condition of the three different pitch regions in the device, highlighting the overlap between the three add-drop windows: the values of the pitch in the three regions have been chosen for this purpose; as it will be shown, this is required to extend the maximum bandwidth of the device.

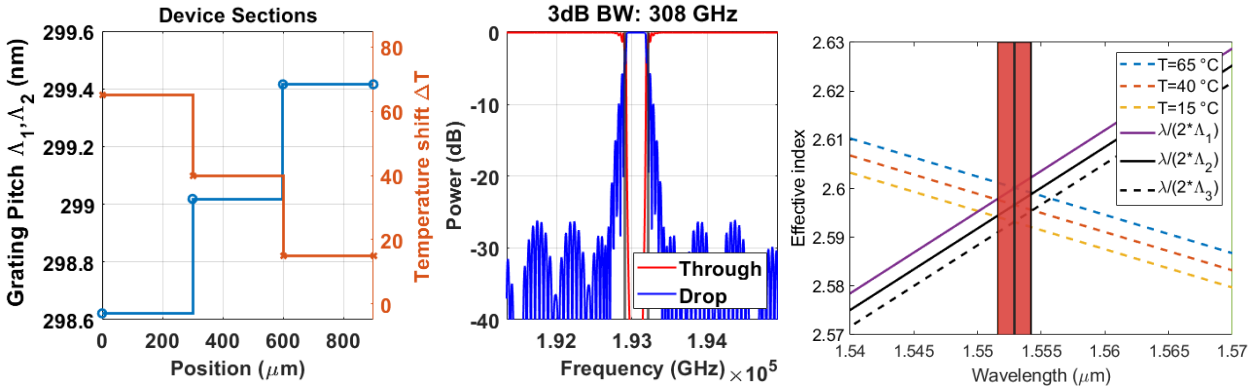

(a) Device regions and resulting response. (b) Phase-match condition.

Figure 3: Minimum bandwidth configuration with negative temperature gradient of $T = [65,\ 40,\ 15]$ °C.

3. THERMAL CONTROL SCHEME

Having described the device and main CMT parameters, adding thermal effects only requires defining the thermo-optic coefficients of the two waveguides, which can be used to apply the appropriate shift to the effective index curves. The two values have been calculated using the RSoft Multiphysics tool, yielding $\mathrm{d}n_1/\mathrm{d}T \approx 1.008 \cdot 10^{-4}$ and $\mathrm{d}n_2/\mathrm{d}T \approx 0.843 \cdot 10^{-4}$, and have been considered constant in frequency and temperature since the analysis is limited to the C-band with temperature ranges $\Delta T = 65\,^{\circ}\mathrm{C}$. It is clear by observing the phase matching condition graph (Fig. 2b) that any shift in the effective index of the waveguides leads to a change in the central frequency of the add-drop window, which can be used in conjunction with the multiple pitch regions to modulate the overlap between the transmission windows, resulting in bandwidth tunability. Fig. 3 depicts the limiting case for the minimum bandwidth, with the highest overlap between the three regions. No further reduction can be obtained, even for larger temperature shifts, as increasing the temperature of the Λ_1 region would move the windows outside of the overlap region, as would decreasing the temperature of the Λ_3 section. Note that the phase-matching figures do not show the spectrum response, but instead the overlap between the ideal square windows introduced by each section: in the actual response, the effect of roll-off factor, the apodization function, and the saturation may leads to spectral difference from the ideal bandwidth of the individual sections.

Analyzing the opposite case further solidifies this concept, illustrating clearly the limiting factor in the thermal scheme. As depicted in Fig. 4a and Fig. 4b, even with the roll-off factor of the actual response, severe notches start to appear in the output response once the windows stop overlapping. By smoothing the thermal gradient along the longitudinal direction, the notches can be compensated, as depicted in Fig. 4c. Nevertheless, this

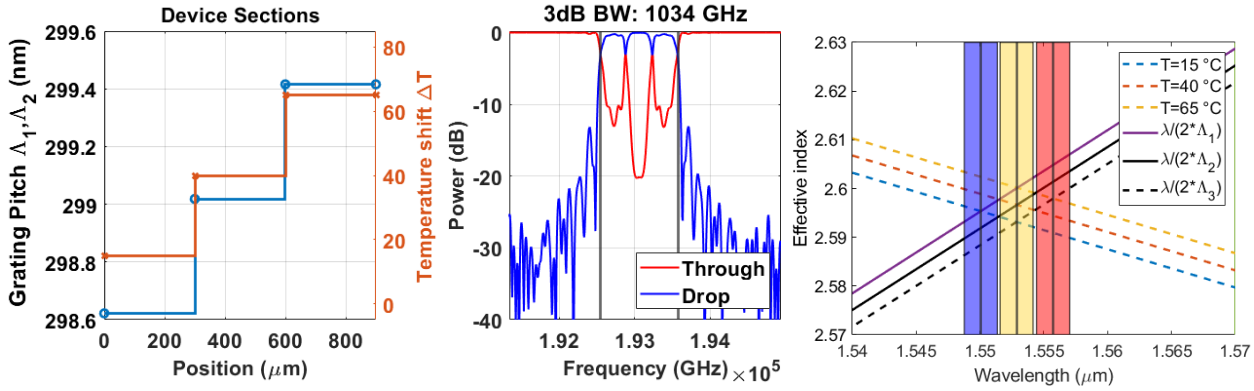

(a) Device regions and resulting response.

(b) Phase-match condition.

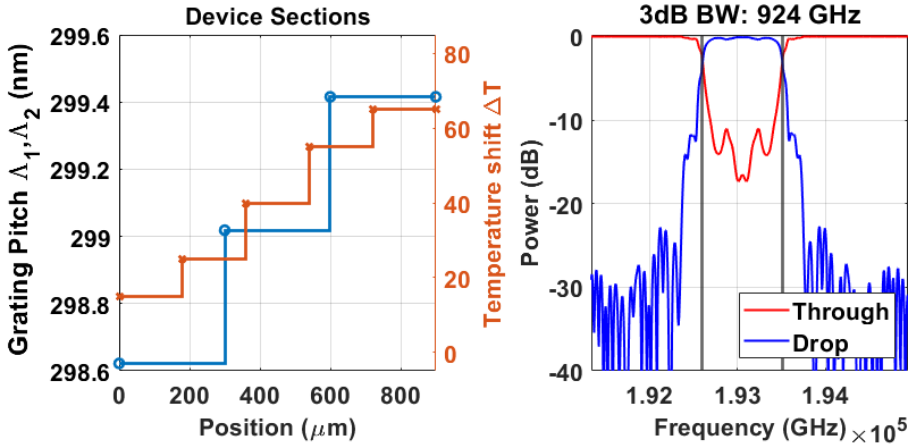

(c) Device regions and resulting response.

Figure 4: (a-b) Nothched configuration, highlighting the gap between the phase-match condition of the regions. (c) Maximum bandwidth configuration with positive temperature gradient of $T = [15,\ 25,\ 40,\ 55,\ 65]\,^{\circ}\mathrm{C}$.

introduces a clear decrease in the bandwidth because of the reduction of the roll-off effect in regions Λ_1 and Λ_3. Moreover this result also highlights the low sensitivity of the system to thermal crosstalk in adjacent regions: due to the main band shifts being provided by the pitch variations, thermal crosstalk can only minimally affect the bandwidth, with a slight reduction of the maximum range and central frequency red-shift, yet without causing notches or severe deformations of the flat-top behavior of the channel.

Considering that the simulated bandwidth of the standalone region is $\Delta f_{3\mathrm{dB}} \approx 335\,\mathrm{GHz}$, the result is in line with the theoretical maximum bandwidth, as the value $\Delta f_{3\mathrm{dB}} \approx 924\,\mathrm{GHz}$ is coherent considering the effects caused by both roll-off and apodization of the side regions. It should be noted that higher temperature ranges coupled with precise gradient profile can increase the maximum bandwidth, especially if the length is further expanded, although the same principle of operation applies: the values of the temperatures have been fixed to a reasonable range, compatible with standard heating seen in the calibration of most silicon photonics device.

4. CONCLUSIONS

We have showcased and analyzed the limits of the bandwidth thermal tuning possibilities for pitch-chirped CDCs, highlighting the principle of operation and simulation-based expected results for a C-band add-drop filter implementation. While the limiting factor for the minimum achievable dynamic bandwidth is confirmed and in line with the expected results, the maximum bandwidth may be further extended by increasing the number of pitch regions, albeit requiring also a higher temperature values, outside the traditional thermal ranges applied in Silicon Photonic circuits control.

ACKNOWLEDGMENTS

This work was supported in part by the US National Science Foundation (NSF) under grant number CNS-2046226.

REFERENCES

[1] Weber, J.-P., "Spectral characteristics of coupled-waveguide bragg-reflection tunable optical filter," *IEE Proceedings J (Optoelectronics)* **140**, 275–284(9) (1993).

[2] Mahdian, M. A., Tunesi, L., Bardella, P., and Nikdast, M., "Bandwidth-adaptive single- and double-channel silicon photonic contra-directional couplers," in [*2023 IEEE Photonics Conference (IPC)*], 1–2 (2023).

[3] Alonso-Ramos, C., Ortega-Monux, A., Zavargo-Peche, L., Halir, R., de Oliva-Rubio, J., Molina-Fernandez, I., Cheben, P., Xu, D.-X., Janz, S., Kim, N., and Lamontagne, B., "Single-etch grating coupler for micrometric silicon rib waveguides," *Opt. Lett.* **36**(14), 2647–2649 (2011).

[4] Shi, W., Wang, X., Zhang, W., Chrostowski, L., and Jaeger, N. A. F., "Contradirectional couplers in silicon-on-insulator rib waveguides," *Opt. Lett.* **36**(20), 3999–4001 (2011).

[5] Tunesi, L., Khan, I., Masood, M. U., Ghillino, E., Curri, V., Carena, A., and Bardella, P., "Design and performance assessment of modular multi-band photonic-integrated WSS," *Opt. Express* **31**(22), 36486–36502 (2023).

[6] Masood, M. U., Khan, I., Tunesi, L., Correia, B., Ghillino, E., Bardella, P., Carena, A., and Curri, V., "Network performance of roadm architecture enabled by novel wideband-integrated wss," in [*GLOBECOM 2022 - 2022 IEEE Global Communications Conference*], 2945–2950 (2022).

[7] Tunesi, L., Khan, I., Masood, M. U., Ghillino, E., Carena, A., Curri, V., and Bardella, P., "Modular photonic-integrated device for multi-band wavelength-selective switching," in [*2022 27th OptoElectronics and Communications Conference (OECC) and 2022 International Conference on Photonics in Switching and Computing (PSC)*], 1–3 (2022).

[8] Shi, W., Wang, X., Lin, C., Yun, H., Liu, Y., Baehr-Jones, T., Hochberg, M., Jaeger, N. A. F., and Chrostowski, L., "Silicon photonic grating-assisted, contra-directional couplers," *Opt. Express* **21**(3), 3633–3650 (2013).

[9] Cauchon, J., St-Yves, J., and Shi, W., "Thermally chirped contra-directional couplers for residueless, bandwidth-tunable bragg filters with fabrication error compensation," *Opt. Lett.* **46**(3), 532–535 (2021).

[10] Hammood, M., Mistry, A., Yun, H., Ma, M., Lin, S., Chrostowski, L., and Jaeger, N. A. F., "Broadband, silicon photonic, optical add–drop filters with 3 dB bandwidths up to 11 THz," *Opt. Lett.* **46**(11), 2738–2741 (2021).

[11] Tunesi, L., Mahdian, M. A., Curri, V., Carena, A., Nikdast, M., and Bardella, P., "Thermal control scheme in contra-directional couplers for centered tunable bandwidths," in [*2023 International Conference on Numerical Simulation of Optoelectronic Devices (NUSOD)*], 115–116 (2023).